

Performance Evaluation of a Printed Circuit Steam Generator for Integral Reactors: A Feasibility Test

Hun Sik Han^{a*}, Han-Ok Kang^a, Juhyeon Yoon^a, Young In Kim^a, Keung Koo Kim^a, Jang-won Seo^b, Brain Choi^b
^aSMART Development Division, Korea Atomic Energy Research Institute, Daedeok-daero 989-111, Yuseong-gu, Daejeon 305-353

^bAlfa Laval Korea Ltd., Techno 8-ro-41, Yuseong-gu, Daejeon, 305-500

*Corresponding author: hshan@kaeri.re.kr

1. Introduction

SMART (System-integrated Modular Advanced Reactor) is a small-sized integral type pressurized water reactor. It adopts advanced design features such as structural safety improvement, system simplification, and component modularization to achieve highly enhanced safety and improved economics. KAERI (Korea Atomic Energy Research Institute) has developed SMART, aiming at exporting it to countries with small electric grids and water supply issues [1]. Recently, the design issues related to further safety enhancement and cost reduction have received significant attention to increase its competitiveness in the global small reactor market. For the cost reduction, it is important to design the reactor vessel as small as possible. Thus, it is necessary to reduce the volume of main components such as a steam generator.

A printed circuit heat exchanger (PCHE) is one of the most promising candidates as a compact heat exchanger. A typical concept of the PCHE manufactured by Heatic Ltd. (UK) is shown in Fig. 1. Its manufacturing processes of the chemical etching and diffusion bonding provide high effectiveness, high compactness, and inherent structural safety under high temperatures and high pressures [2]. Thus, it is expected to be an alternative to the conventional shell and tube type steam generator in SMART. In this paper, simple thermal-hydraulic performance measurement of a small-scale printed circuit steam generator (PCSG) is conducted to investigate the feasibility of applying it to SMART.

2. Experimental Setup and Procedure

The experimental setup was composed of a closed oil loop and an open water loop for the hot and cold sides, respectively, as shown in Fig. 2. A PCSG was employed for a performance test. The PCSG consisted of one cold side plate and two hot side plates, and each plate had 26 micro-wavy channels of 2 mm in width and 0.8 mm in depth with a semi-elliptical cross sectional shape.

Considering that a higher flow rate is required in the hot side compared to the cold side for SMART operation, a double-banking design, which stacks one cold side plate with two hot side plates in a sandwich structure [3, 4], was adopted. Also, the 2-dimensional flow channel design was applied to the cold side plate,

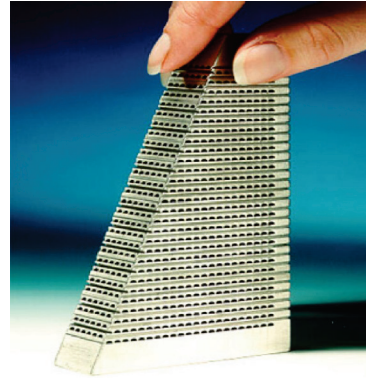


Fig. 1. Printed circuit heat exchanger (Heatic Ltd.).

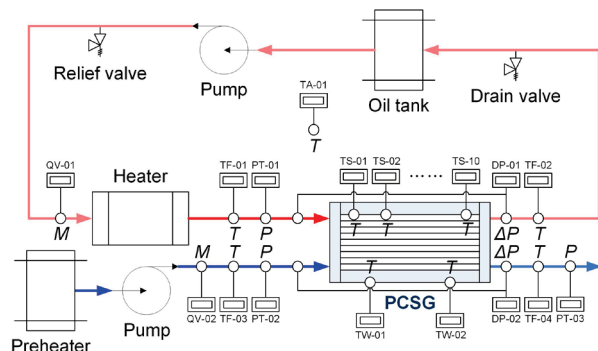


Fig. 2. Schematic diagram of the experimental setup.

while the hot side plates were equipped with 3-dimensional flow channels. In the 2-dimensional flow channel design, the channels are fabricated on only one side of the plate with honeycomb patterns, and thus flow mixing is allowed between the neighboring channels. In the 3-dimensional flow channel design, on the other hand, both sides of the plate have the honeycomb type flow channels, and the through holes patterned periodically along the flow path enable the additional flow mixing between the upper side and bottom side channels. The plate dimension was 600 mm × 150 mm, as highlighted in Fig. 3.

The thermal oil heated by a 20 kW electric heater flowed into the hot side of the PCSG, and released thermal energy into the cold side. As the water traveled along the flow path of the PCSG, it absorbed heat from the thermal oil and began to evaporate. The superheated steam was then vented out. Experiments were performed under counter flow conditions, and the experimental

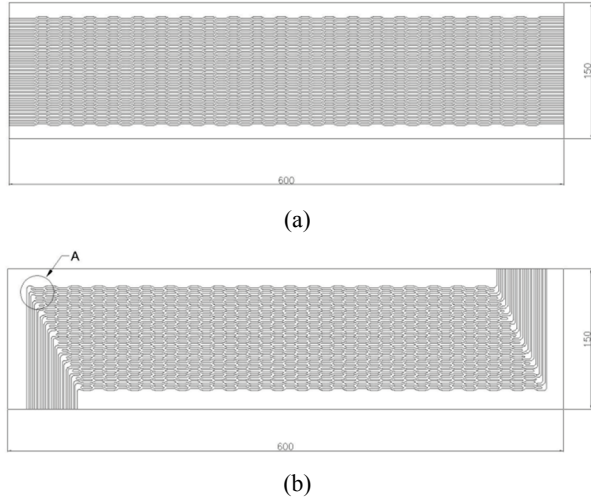


Fig. 3. Flow channel configuration: (a) hot side plate and (b) cold side plate.

data were stored in a data acquisition device with a 1-Hz sampling frequency after reaching a time-periodic quasi steady-state.

In an effort to obtain consistent experimental data, the following procedure was adopted during the start-up and performance measurement. At the beginning of the experiment, the PCSG was preheated for 30 min to remove non-condensable gas from the cold side. After reaching a steady-state, the experimental data such as temperatures, pressures, pressure drops, and flow rates were measured. In the present study, the PCSG was regarded as being in the time-periodic quasi steady-state when the temperatures were well within a range of $\pm 1^\circ\text{C}$ from the time-averaged value for at least 5 minutes except for the cold side inlet temperature. The parameter ranges were $0.1 \text{ lpm} \leq m_c \leq 0.3 \text{ lpm}$, $m_h = 25 \text{ lpm}$, and $p_{\text{c,out}} = 1 \text{ bar}_{\text{gage}}$.

3. Data Reduction

To process the experimental data, it is useful to introduce the dimensionless quantities as follows:

$$T = \frac{t}{t_{\text{sat}@p_{\text{c,out}}}}, \quad (1)$$

$$P_c = \frac{p_c}{p_{\text{c,out}}}, \quad (2)$$

$$\Delta P_c = \frac{\Delta p_c}{\Delta p_{\text{cref}}}, \quad (3)$$

$$Q_c = \frac{q_c}{q_{\text{cref}}}. \quad (4)$$

In the above, $t_{\text{sat}@p_{\text{c,out}}}$ is the saturation temperature of water at a given pressure, $p_{\text{c,out}}$ is the cold side outlet pressure, Δp_{cref} is the reference value of the cold side pressure drop through the PCSG, and q_{cref} is the reference value of the cold side heat transfer rate. The heat transfer rates of the hot and cold sides are given as

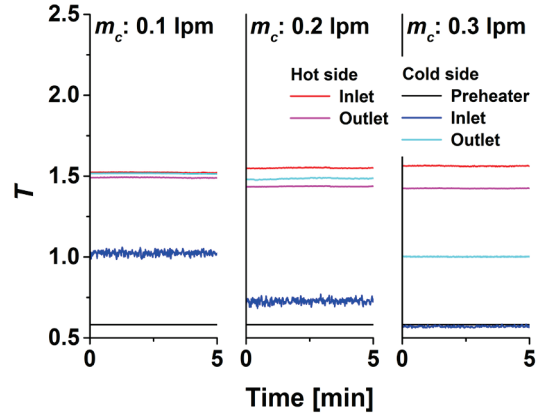
$$q_h = m_h C_p (t_{\text{hin}} - t_{\text{hout}}), \quad (5)$$

$$q_c = m_c (i_{\text{c,out}} - i_{\text{c,in}}), \quad (6)$$

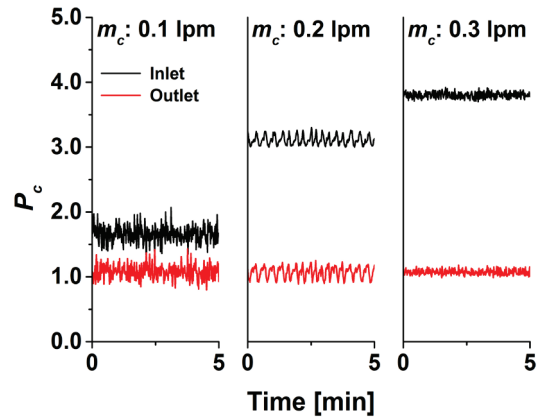
where C_p is the specific heat of thermal oil and i is the enthalpy of water.

4. Results and Discussion

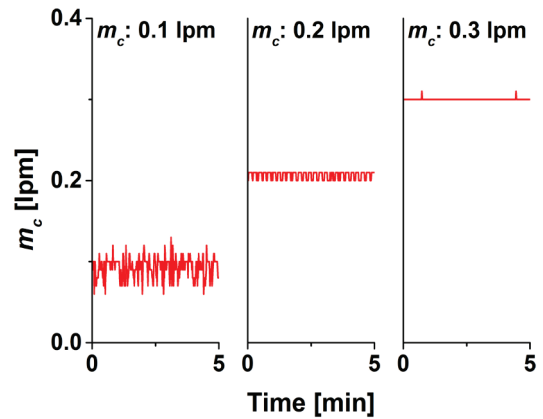
The measured temperatures of the PCSG are displayed in Fig. 4a. The PCSG shows typical temperature distributions in the counter flow heat exchanger. As can be seen in the case of $m_c \approx 0.1 \text{ lpm}$,



(a)



(b)



(c)

Fig. 4. Time history of the measured parameters: (a) temperature, (b) cold side pressure, and (c) water flow rate.

the PCSG generates superheated steam stably. As the water flow rate increases, however, the degree of superheat decreases, and the saturated liquid-vapor mixture is vented out when the flow rate increases to 0.3 lpm. In addition, the cold side inlet temperature shows fluctuating behavior and is much higher than the preheating temperature when the water flow rate is low. As the flow rate increases from 0.1 lpm to 0.3 lpm, however, it approaches the preheating value and the fluctuating trend almost disappears.

This is attributed to the fact that there are reverse flows due to density-wave oscillation in the PCSG core when the phase changes occur intensively. Thus, the inlet temperature becomes higher than the preheating temperature and fluctuates. Here, the cold side inlet temperature in the case of $m_c \approx 0.3$ lpm is slightly lower than the preheating temperature because the water temperature decreases as the water flows along the pipe due to the heat loss.

Figs. 4b and c exhibit the variation of the cold side pressures and water flow rates, respectively. As expected, the pressure drop increases with the increment in the water flow rate. It is discernible that the density-wave oscillation is decreased with a decline in the degree of superheat by increasing the water flow rate. To prevent such a flow reversal phenomenon due to the phase change, it is required to apply the orifice channel to the cold side. Such a density wave oscillations are suppressed due to a strong stabilizing effect of the added single-phase resistance [5].

The time-averaged cold side pressure drops and heat transfer rates at various water flow rates are presented in Fig. 5. The pressure drops and heat transfer rates are non-dimensionalized using a reference value of Δp_{cref} and q_{cref} , respectively. Here, the pressure drop and heat transfer rate when the water flow rate is almost 0.1 lpm in the non-orifice PCSG is selected as the reference values. The higher water flow rate brings forth the augmented the pressure drop and heat transfer rate. It is noted that heat transfer rate is enhanced at the expense of the large pressure drop. Here, the cold side heat

transfer rates evaluated from Eq. (6) are consistent with the hot side heat transfer rate given by Eq. (5) within $\pm 10\%$ relative deviation.

5. Conclusions

The simple thermal-hydraulic performance of the PCSG has been experimentally evaluated. A small-scale PCHE is employed to investigate the feasibility of operating it as a steam generator. The performance assessment reveals that the PCSG stably produces superheated steam, and the increased degree of superheat is obtained at lower water flow rate. However, the flow instability is increased with the decrease of the water flow rate. Thus, it is required to apply the orifice design into the cold side plate to suppress the density-wave oscillations. The pressure drops and heat transfer rates increase with the water flow rate.

ACKNOWLEDGEMENT

This work was supported by the National Research Foundation of Korea (NRF) funded by the Ministry of Science, ICT and Future Planning (No. NRF-2012M2A8A4025974), South Korea.

REFERENCES

- [1] K. K. Kim, W. Lee, S. Choi, H. R. Kim, and J. Ha, SMART: The First Licensed Advanced Integral Reactor, *Journal of Energy and Power Engineering*, Vol.8, p.94, 2014.
- [2] Q. Li, G. Flamant, X. Yuan, P. Neveu, and L. Luo, Compact Heat Exchangers: A Review and Future Applications for a New Generation of High Temperature Solar Receivers, *Renewable and Sustainable Energy Reviews*, Vol.15, p.4855, 2011.
- [3] K. Nikitin, Y. Kato, L. Ngo, Printed Circuit Heat Exchanger Thermal-Hydraulic Performance in Supercritical CO₂ Experimental Loop, *International Journal of Refrigeration*, Vol.29, p.807, 2006.
- [4] T. L. Ngo, Y. Kato, K. Nikitin, N. Tsuzuki, New Printed Circuit Heat Exchanger with S-Shaped Fins for Hot Water Supplier, Vol.30, p.811, 2006.
- [5] R. T. Lahey, Jr., F. J. Moody, *The Thermal-Hydraulics of a Boiling Water Nuclear Reactor*, American Nuclear Society, 1997.

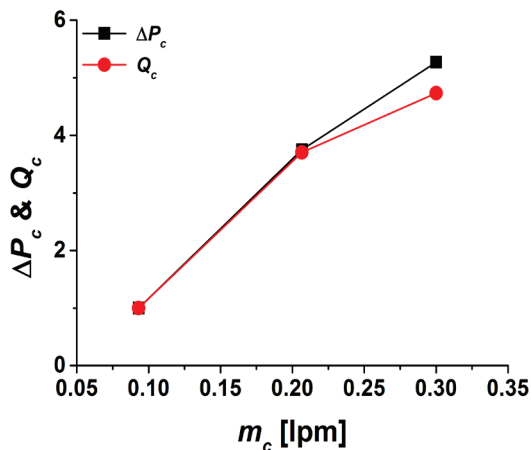


Fig. 5. Pressure drop and heat transfer rate in the cold side versus the water flow rate.